Anal. Chem. **2007,** *79,* 702−709

Differential Surface Plasmon Resonance Imaging for High-Throughput Bioanalyses

Daniel Boecker,[†] Alexander Zybin,*[,†] Vlasta Horvatic,[†,§] Christian Grunwald,[‡] and Kay Niemax[†]

ISAS - Institute for Analytical Sciences at the University of Dortmund, Bunsen-Kirchhoff-Str. 11, D-44139 Dortmund, Germany, and Max-Planck-Institute for Molecular Physiology, Otto-Hahn-Str. 11, D-44202 Dortmund, Germany

A new imaging technique for high-throughput surface plasmon resonance (SPR) measurements is described. It is the application of a CCD camera for simultaneous processing of two images at two different wavelengths provided by two laser diodes. The two lasers are brought to resonance by tuning of the angle of incidence so that the detection power and the dynamic range are optimized for the wavelength pair selected. Applying a special differential processing of the two images, SPR measurements can be performed near the shot noise limit taking into account the number of CCD pixels involved. It is shown that the detection limit of imaging methods can be improved significantly if the working point is set near to the reflection minimum instead of choosing the angle with the steepest slope of the reflection curve. The technique is demonstrated by simultaneous measurement of hybridization reactions of three different types of thiolated oligonucleotides in 30 small areas set by a commercial spotter. A noise level of 1.5×10^{-6} refractive index units (RIU) was obtained for single, 500×500 μm^2 reaction areas. The noise level was about 6×10^{-7} RIU when five areas were taken into account. The present arrangement and the particular spotter applied would allow simultaneous measurements of up to 400 binding reactions with a noise level of about 1.5×10^{-6} RIU.

Significant progress has been made in the field of surface plasmon resonance (SPR) detection of biomolecules after its first application.[1] In particular, the commercialization of the method and numerous applications in pharmacology, proteomics, and bioanalysis have stimulated an intensive development of the SPR method and led to important improvements of the technique. Modern SPR devices are able to detect binding of molecules with densities of about 100 pg/cm^2 on the surfaces. This corresponds to a variation of the effective layer thickness of about 1 pm (see, e.g., ref 2) or a variation of the volume refractive index $\Delta n \sim 10^{-6}$. The quoted sensitivity is sufficient to detect even the binding of small molecules (∼100 Da) to antibodies[3] and fulfills the requirements for almost all important applications. A very important option of SPR-based methods is the possibility of high-throughput analyses. SPR imaging provides the possibility to detect simultaneously hundreds of different reactions if biomolecules are immobilized on designated spots some few tens of micrometers wide. However, the development of SPR instruments for high-throughput with low detection limits is still a challenging task.

Several concepts for SPR imaging have been studied recently. The most straightforward concept uses illumination of the sensor surface by a parallel monochromatic beam with an incidence angle slightly shifted from the resonance minimum to the wing of the resonance curve. The reflected beam is monitored by a CCD camera so that a reflectivity distribution across the sensor surface can be quantified. Molecular binding reactions at the surface are causing shifts of the resonance curve and hence a change of the reflectivity. Therefore, the variations of the reflectivity measured by the CCD camera deliver information about ongoing binding processes at the surface. However, by using such an arrangement, intensity drifts and fluctuations due to absorption or scattering are contributing to the noise. The mentioned arrangement, being very simple, has demonstrated detection limits (3σ-criterion) not better than $\Delta n \approx 3 \times 10^{-5}$ even for relatively large spots.[4]

Another interesting concept examined for SPR imaging is based on the measurement of phase shifts of the reflected beam[5−7] instead of intensity detection. This method promises low detection limits. Here, the interference of the SPR beam with a reference beam is used to reveal phase shifts and to transform them into intensity variations. Several groups reported interference-based measurements; however, fringe analysis especially for imaging is still difficult, and the detection power is reduced if reactions in small spots on the surface are measured.[8,9]

The differential imaging method described in the present paper provides an opportunity to reduce factors which derogate the detection limit of single-wavelength imaging methods. Here,

* To whom correspondence should be addressed. E-mail: zybin@isas.de.
† ISAS - Institute for Analytical Sciences at the University of Dortmund.
‡ Max-Planck-Institute for Molecular Physiology.
§ Permanent address: Institute of Physics, Bijenicka 46, 10000 Zagreb, Croatia.

(1) Liedberg, B.; Nylander, C.; Lundström, I. *Biosens. Bioelectron.* **1995**, *10*, I−IX.
(2) Stenberg, E.; Persson, B.; Roos, H.; Urbaniczky, C. *J. Colloid Interface Sci.* **1991**, *143*, 513.
(3) http://www.biacore.com/lifesciences/index.html.
(4) Shumaker-Parry, J. S.; Campbell, C. T. *Anal. Chem.* **2004**, *76*, 907.
(5) Kabashin, A. V.; Nikitin, P. I. *Opt. Commun.* **1998,** *150,* 5.
(6) Nikitin, P. I.; Beloglasov, A. A.; Grigorenko, A. N.; Kochergin, V. E; Valeiko, M. V.; Ksenevich, T. I. *Sens. Actuators, B* **1999**, *54*, 43.
(7) Nikitin, P. I.; Grigorenko, A. N.; Beloglasov, A. A.; Valeiko, M. V.; Savchuk, A. I.; Savchuk, O. A.; Steiner, G.; Kuhne, C.; Huebner, A.; Salzer, R. *Sens. Actuators, B* **2000**, *85*, 189.
(8) Chen, S.-J.; Su, Y.-D.; Hsiu, F.-M.; Tsou, C.-Y.; Chen, Y.-K. *J. Biomed. Opt.* **2005**, *10* (3), 034005.
(9) Piliarik, M.; Vaisocherov'a, H.; Homola, J. *Biosens. Bioelectron.* **2005**, *20*, 2104.

10.1021/ac061623j CCC: $37.00
Published on Web 11/15/2006

an additional second laser with a different wavelength for differential image processing is applied which allows us to obtain low detection limits in relatively small spots. This means that the new technique is suitable for sensitive high-throughput measurements.

CONCEPT OF DIFFERENTIAL SPR IMAGING

The simplest and most often applied SPR imaging technique is based on intensity measurements at a fixed reflection angle. The surface is illuminated by a collimated monochromatic beam slightly shifted from the SPR resonance angle to the wing of the resonance curve, so that any shift of the resonance is causing a change of the reflected intensity. The intensity variations due to molecular binding in different spots on the surface can be observed simultaneously by means of a CCD matrix.[4] Being very simple, this technique can be affected by possible changes of the resonance curve due to unexpected modification of the surface roughness or to light absorption. Light diffracted and/or scattered by the optical surfaces can also interfere with the radiation reflected from the spots and, therefore, deteriorate the detection power. This is especially critical if miniaturized, high-capacity arrays with small spots are used. Therefore, this technique is generally less sensitive than the angle-based technique applied usually in single-spot measurements of large areas.

Recently, a new concept for SPR imaging has been demonstrated at ISAS.[10] It applies two widened, collimated laser beams of different wavelengths combined in one beam irradiating the metal surface of the SPR device. The spatial intensity distribution of both beams should be as similar to each other as possible. The wavelengths of the lasers are tuned to the opposite sides of the SPR curve. The reflected intensities of the laser beams can be made equal by fine-adjusting of the incidence angle which results in equal photodetector currents for both wavelengths. During the measurement the lasers are alternatively switched on and off with a frequency of a few kilohertz, so that always only one of the lasers is operating at a time. In this mode, the photodetector measuring the reflected intensities produces a direct-current (dc) signal. Any shift of the SPR curve results in a difference of the reflectivity of both wavelengths and gives rise to an alternating-current (ac) signal of the photodiode. The value of the ac component can be used to characterize the shift and, therefore, the adsorption processes in the layer adjoined to the gold surface. This technique can be applied in imaging mode and has shown detection limits on a few spots which are comparable with the best detection limits of non-imaging SPR techniques.

Wavelength Optimization for Differential Imaging. To find the best wavelengths for differential SPR measurements, the *SPR 4 Phase Fresnel Reflectivity Online-Calculation*[11] was used. The sensitivity is defined as $\mathrm{d}R/\mathrm{d}n$, (R represents reflectivity). It characterizes the slope of the reflectivity curve and is often used for optimization in SPR measurements.[12] The angle corresponding to the maximum sensitivity provides a maximum signal if Δn is varied. This procedure allows us to find the parameters for a maximum signal but not for the maximum detection power. Therefore, the optimization of the detection power should take into account not only the measured signal but also the signal-to-noise ratio. One obtains, certainly, other values for the optimal angle if the S/N ratio instead of the signal alone is taken into account. The optimization of the S/N ratio was discussed in ref 13 for the single-wavelength detection; however, the optimum incident angle was not derived. In the present work, the S/N-based approach is applied for optimizing of both single- and double-wavelength detection schemes.

The signal caused by a given variation of Δn can be expressed as

$$S = \eta I_0 (\mathrm{d}R/\mathrm{d}n)\Delta n \tag{1}$$

where η is the quantum efficiency of the photo detector, and I_0 is the illumination intensity.

The shot noise can be given as

$$N = \sqrt{\eta I_0 R} \tag{2}$$

Therefore, the S/N ratio is

$$S/N = \sqrt{\eta I_0 / R}(\mathrm{d}R/\mathrm{d}n)\Delta n \tag{3}$$

Since both R and $\mathrm{d}R/\mathrm{d}n$ are wavelength- and angle-dependent,

$$\frac{\mathrm{d}R/\mathrm{d}n}{\sqrt{R}} \tag{4}$$

should be considered in the optimization procedure to find the best wavelength or incidence angle for a constant illumination intensity.

An interesting situation arises if imaging with a CCD is applied. In this case, the intensity can be increased only until the pixels are saturated by the reflected light. It means that the optimum illumination intensity depends on the reflectivity. In the case of low reflection, high-illumination intensities should be applied. The optimum intensity

$$I_{\mathrm{opt}} = I_\gamma / R \tag{5}$$

where I_γ is an intensity slightly below the CCD saturation intensity, for example, 90% of the saturation intensity.

Applying a laser illuminating source with a few milliwatts intensity and a detector with 10^6 pixels, one can measure $>10^8$ photons/s per pixel at 1% reflectivity. This is sufficient for any modern CCD chip to be saturated, so that the intensity has to be reduced anyway.

(10) Zybin, A.; Grunwald, C.; Mirsky, V. M.; Kuhlmann, J.; Wolfbeis, O. S.; Niemax, K. *Anal. Chem.* **2005,** *77*, 2393.
(11) http://unicorn.ps.uci.edu/calculations/fresnel/fcform.html.
(12) Johansen, K.; Arwin, H.; Lundström, I.; Liedberg, B. *Rev. Sci. Instrum.* **2000**, *71*, 3530.
(13) Chinowsky, T. M.; Mactutis, T.; Fu, E.; Yager, P. *Proc. SPIE* **2004**, *5261*, 173.

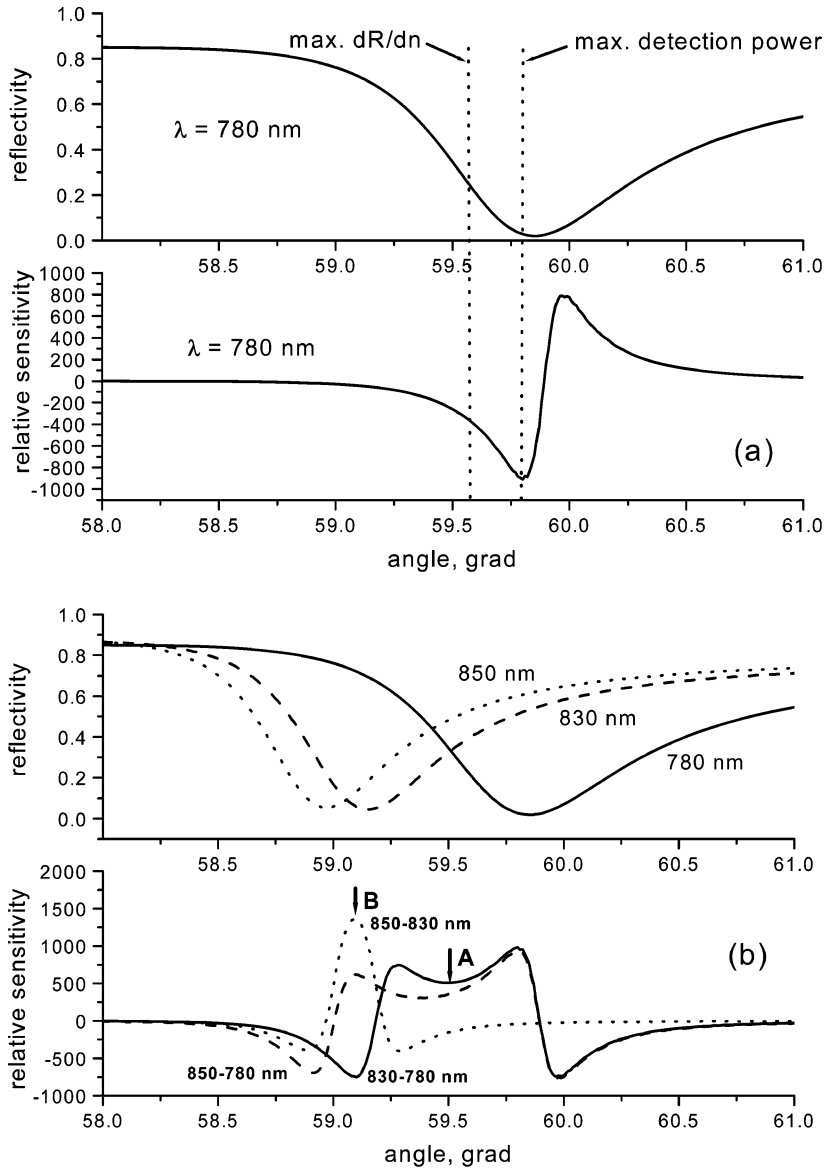

Figure 1. (a) Theoretical SPR reflectivity (top) and relative SPR sensitivity (bottom) for $\lambda = 780$ nm in dependence on the angle of incidence. (b) Theoretical SPR reflectivity for three different laser wavelengths (top) and the relative SPR sensitivities applying the differential method with three different wavelength pairs (bottom), both in dependence on the angle of incidence. Positions A and B in the bottom figure are explained in the text.

Therefore, the optimum S/N ratio is given by

$$S/N = \sqrt{\eta I_\gamma}\frac{\mathrm{d}R/\mathrm{d}n}{R}\Delta n \tag{6}$$

where

$$E = \frac{\mathrm{d}R/\mathrm{d}n}{R} \tag{7}$$

is the parameter to be optimized by the choice of the wavelength or the incidence angle. In the following, E is named relative sensitivity. As can be seen in Figure 1a, the optimum detection power is obtained not in the steepest part of the reflection curve but near to the minimum. The S/N ratio is better than a factor of about 2 by taking into account the optimum angle instead of the angle at the point where the reflection curve has its steepest slope. The reason is that the reflectivity R in the denominator of eq 7 is reducing more rapidly than the slope $\mathrm{d}R/\mathrm{d}n$ in the numerator if the incident angle is varied from the steepest part of the resonance curve to the minimum.

It is interesting to note that the same value E as in eq 7 should be used for optimization of the detection power if the noise is directly proportional to the intensity. This is the case, for example, when fluctuations of the source intensity are dominating the noise. Here, the noise can be written as $N = \alpha\eta I_0 R$ (α is a proportionality coefficient)

$$S/N = \alpha^{-1}\frac{\mathrm{d}R/\mathrm{d}n}{R}\Delta n \tag{8}$$

and depends only on E for both types of detectors—photodiode and CCD camera.

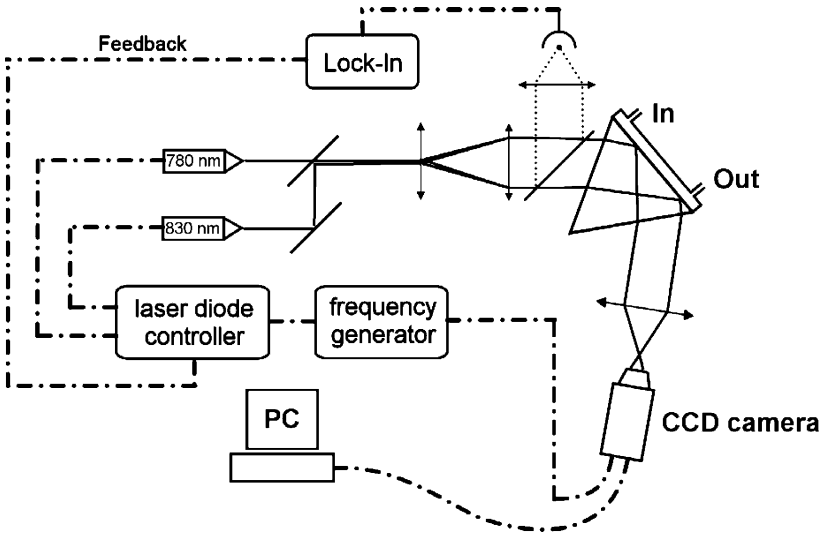

Figure 2. Experimental arrangement.

It must be pointed out that the useful dynamic range is very small if the experiment is run at optimum detection conditions. Therefore, the working point should be shifted slightly from that position to increase the dynamic range. For example, the lower plot of Figure 1a shows the calculated dependence of the relative sensitivity E on incident angle for a laser wavelength of 780 nm. E has an extremum at about 59.8° near to the minimum of the SPR reflectivity curve shown in the upper part of Figure 1a. However, as mentioned above, the useful dynamic range at that position is very small when the SPR resonance curve is shifting. Therefore, a choice of an angle slightly shifted toward smaller values, for example, to 59.75°, where the relative sensitivity is ~800 RIU^{-1}, would be better. It has to be noted that the conclusions are valid only in the absence of background radiation. This should be taken into account if the experiment is optimized.

The described optimization procedure can also be applied if two lasers with different wavelengths are used. In the lower part of Figure 1b, the calculated detection sensitivities in dependence on the incident angle are displayed if differential SPR with selected wavelength pairs is applied. The upper curves in Figure 1b show the experimental reflectivity curves of the chosen wavelengths (780, 830, and 850 nm). In the present work, the wavelength pair 830−780 nm was mainly used. At 59.5°, the measured relative sensitivity with this pair was found to be about 500 RIU^{-1} which is in a good agreement with theoretical datum indicated by point A in Figure 1b. Higher relative sensitivity can be achieved if pairs with close-lying wavelengths are used. For example, the pair 850−830 nm provides a three times better relative sensitivity at point B in Figure 1b than 830−780 nm, but the dynamic range is much smaller. As already stated, pair 830−780 nm was used in the present work in order to have a sufficiently large dynamic range. This is important for testing the method. A final SPR imaging instrument should have two options: one for high-sensitivity measurements, where the dynamic range is not important, and the second one for measurements with a large dynamic range. This can be easily realized by using an additional laser diode.

INSTRUMENTATION

The experimental arrangement is shown in Figure 2. Radiation

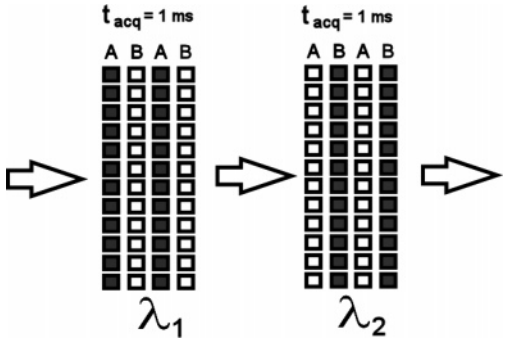

Figure 3. Operation principle of differential SPR with two laser wavelengths applying a modified CCD for detection. The active pixel sets A and B are switching synchronously with the respective lasers.

in two laser diodes (GHO781JA2C from Sharp and HL-8325G from Hitachi) at 780 and 830 nm respectively, was combined in one beam by means of a beam splitter. The overlapping beams were expanded to a diameter of about 3 cm (fwhm) and used for illumination of the SPR prism. The dimension of the input face of the prism was 2 × 1 cm^2. The inhomogeneity of the intensity across the surface was of about 30%. Both laser diodes were driven by commercial power supplies (type ITC-502, Profile, Germany).

The SPR flow cell consisted of a plexiglas block on one and the gold-coated prism on the other side separated by a 300-μm-thick rubber seal which formed an S-shaped flow channel. The volume of the flow cell was about 60 μL. A peristaltic pump was used to provide a buffer flow through the flat flow cell. A glass lens with $f = 5$ cm was used to image the SPR surface on the CCD camera. Two modified cameras were used: MV 14-205 (company: Soliton, Gilching, Germany) with a pixel capacity of 13600 electrons per pixel and MV 14-285 (also from Soliton) with 36000 electrons per pixel. Both CCD chips had 1024 × 1360 pixels. Each camera offers the possibility to record and compare two images quasi-simultaneously. Two sets of pixel lines (A and B), as shown in Figure 3, were triggered alternatively with a frequency up to 15 kHz so that during each half-period only one set of pixels is sensitive for illumination. Since the lasers are switching synchronously, each pixel set receives only the irradiation of the

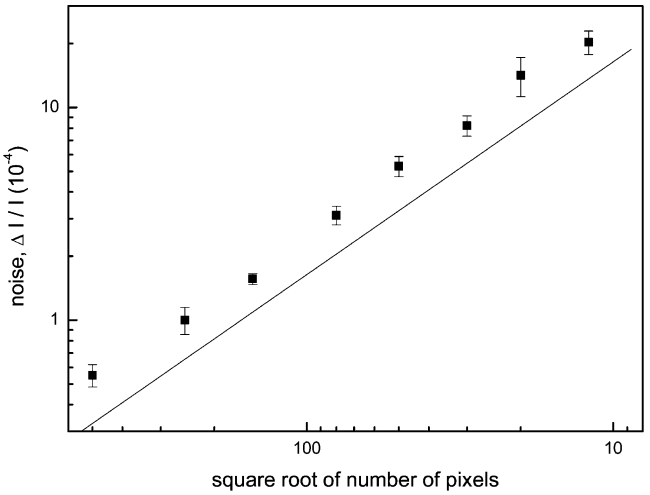

Figure 4. Experimental noise in dependence on the inverse number of CCD pixels illuminated by one laser wavelength. The straight line represents the calculated shot noise taking into account the experimental conditions.

corresponding wavelength. After each half-period, the charges of the corresponding pixel sets are transferred into the interline register on the CCD chip where the charges of many measurement cycles are accumulated. After the exposure, the integrated charge is converted with a 14-bit resolution into a digital signal and transferred to the PC by a frame grabber for further processing. A readout frequency of 2 Hz was applied although the camera allows, in principle, readout frequencies up to 5 Hz. The limitation was due to the homemade program which calculated the mean values for both pixel sets separately for several beforehand-designated areas of the image. The intensities of both wavelengths and the difference of the signals can be plotted in real time for all areas. This allows the measurement of binding events in different spots on the surface in real time with all advantages of the two-wavelength differential SPR technique discussed in our previous paper.[10]

An active feedback loop could be used to equalize the intensities of both lasers. For this purpose, a fraction of the combined laser beam intensity was taken by means of a beam splitter and guided to a photodiode. The alternating current (ac) component of the photodiode current was fed into a lock-in amplifier. The output signal of the lock-in amplifier was applied to the diode laser diode drivers to equalize the laser intensities.

CCD-Camera Noise. CCD cameras have excess noise due to dark current and readout noise. In order to measure this noise, the CCD was illuminated by an expanded beam of a continuous-wave laser diode. Several areas of different size on the CCD chip were taken into account for this investigation. The signals of A and B pixel sets were integrated separately, and a difference signal was calculated for each defined area. Since the intensities on both pixels sets are the same, the differential signal is a measure of shot noise and camera excess noise. Figure 4 shows the differential noise in dependence on the size of the pixel area. As can be seen, the measured noise signals exceed only slightly the theoretically expected shot noise level presented by the straight line. Taking the experimental results into account, it turns out that the noise of the CCD can be neglected if the number of collected photoelectrons per pixel is not smaller than 50% of the saturation value.

Samples and Surface Preparation. Protein (N-Ras(1-181)) and oligonucleotides, each containing thiol links, were used as test samples. The protein was stored in 20 mM potassium phosphate buffer containing 5 mM $MgCl_2$ (pH = 7.4). The concentration was 20 g/L. The protein was diluted with water in the relation 1:1 for the spotting process. The oligonucleotides were diluted in 10 mM KH_2PO_4 and 100 mM KCl buffer (pH = 6.5). The concentration was 1 μM (T1-HCV, T2-HCV, G-HCV) or 2 μM (RS1-HCV, RS2-HCV).

The prototype of a commercial spotter (TopSpot by BioFluidiX, Freiburg, Germany) was used to generate the SPR detection arrays. Drops of 17 nL containing thiol-linked molecules were spotted onto destined places at the surface. During the spotting process, which took about 1 min, the gold slide was cooled to about 10 °C. After spotting, the gold slide was placed in a closed container with a high humidity. This is necessary to protect the small droplets against evaporation. After 30 min, the gold slide was rinsed with water and dried with nitrogen.

RESULTS AND DISCUSSION

Limitations in SPR Imaging. Lasers provide usually enough radiation that the shot noise of the light source is smaller than other noise sources in the experiment. Unfortunately, it is not possible to take advantage of the high radiation power delivered by lasers because the pixel capacities of a CCD chip are limited. For example, choosing a relative sensitivity of 800 for single-wavelength detection, the shot noise limit is $(\Delta I/I) = 4 \times 10^{-3}$ or $\Delta n \sim 5 \times 10^{-6}$ for a single pixel if the electron capacity of single pixels is about 3×10^4 and a readout frequency of 2 Hz is used. For example, the noise level can be reduced to $\Delta n \sim 3 \times 10^{-7}$ if the charges of 400 pixels are summed up. This is comparable with the detection power of the most powerful commercial SPR instruments analyzing up to four areas on a surface.[3]

The shot noise of SPR detection with two wavelengths is three times larger because only half of all pixels are available for each wavelength and the noise signals of both pixels are adding up if the signals are subtracted. However, the signal is almost twice as large as with one wavelength because the signals are adding up as well.

Taking into account the necessary space between the reaction areas, the total area necessary for a single reaction spot, containing 400 pixels, is 1600 pixels. Therefore, about 1000 reactions can be monitored simultaneously by means of a CCD chip containing 1.6×10^6 pixels. In this case, the measurement areas provide a noise level of about 3×10^{-7} RIU as discussed above. This rough estimate supposes that shot noise is the limiting factor. The analytical power decreases if other noises are dominating. This can often be observed. It has to be noted that shot noise is dominating if the spots are very small. In general, high-throughput application is at the expense of detection power.

It should be noted that the signal derived from the area between hybridization spots can be used as reference. By this it is possible to reduce significantly the noise caused by temperature variations and mechanical drift and/or vibration and to improve the detection limit. Therefore, hybridization measurements in single spots were performed to evaluate the detection power of the technique rather than volume refractive index measurements.

Stabilization of the Intensity. The intensity instability of the laser beam ($\Delta I/I$) is one of the major sources of noises for SPR

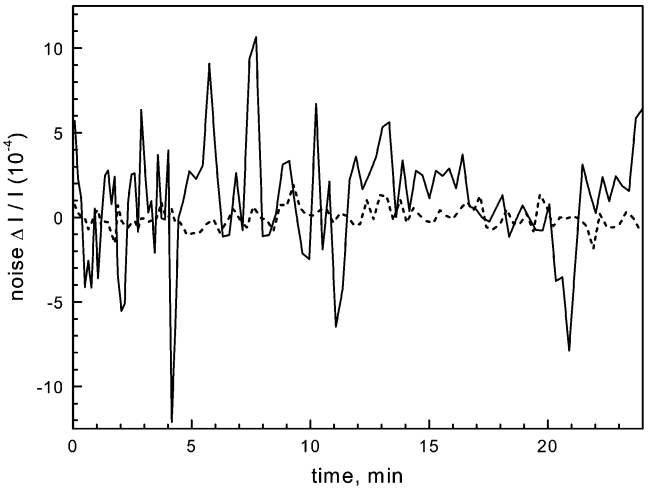

Figure 5. Intensity fluctuations of the SPR difference signal measured with (dashed line) and without feedback (full line) for intensity equalization of the two laser beams.

imaging since each fluctuation of the laser intensity is directly contributing to the noise. In SPR measurements with two wavelengths, the CCD chip is illuminated by two different lasers. The fluctuations of both lasers are not correlated and cause significant noise in the difference signal. The fluctuations can be reduced by active intensity adaptation of both laser beams as described in detail in our previous paper.[11] In brief, the difference signal at the modulation frequency has to be fed into a lock-in amplifier, and the analog-output current of the lock-in amplifier is applied as a negative feedback signal to the current of one of the laser diodes. As shown in Figure 5, the intensity adaptation improved the stability of the differential signal by a factor of about 5. In the present experiment, the differential signal was measured by means of a CCD camera. It should be noted here that the laser diode should operate in single mode. The operation is unstable if the laser diode current is near to a mode hop[14] and modes with different wavelengths are randomly generated in each modulation cycle. Here the feedback loop is ineffective. Stable operation conditions can be expected only in working ranges far from a mode hop.

Simultaneous Monitoring of Oligonucleotide Hybridization. To check the high-throughput capability of the present SPR arrangement, a DNA array was prepared on the gold surface as described above. Five different oligonucleotides and one protein (N-Ras(1-181)) were used (see Table 1). All molecules were attached to the gold surface using thiol links.

The diameters of the spots were 480 ± 50 μm, and the spot-to-spot distance was about 800 μm. This corresponds to about 30% cover of the whole imaged surface by DNA (25%) and proteins (5%). The protein was used as a marker because it causes, in contrast to the DNA used, large SPR shifts and helps to find the DNA spots on the gold surface. A section of the array pattern is shown in Figure 6. Unfortunately, the prototype spotter did not provide a perfect spot array. Some spots were not placed on their designated position or were not set at all. This has to be taken into account when benchmarking the experimental results below. The size of the whole array was 2 × 2 cm^2. Depending on the

(14) Franzke, J.; Schnell, A.; Niemax, K. *Spectrochim. Acta Rev.* **1993**, *15*, 379.

Table 1. Oligonucleotides Immobilized on the Gold Surface by Thiol Links and the Analytes with Complementary Sequences

symbol	sequence (5′-3′)
RS1-HCV	HS-(CH)$_6$–TTT TTA GAA GAC AAA GAG CTC AT
RS2-HCV	HS-(CH)$_6$–TTT TTA GAA GAG AAA GAG CTC AT
T1-HCV	HS-(CH)$_6$–TTT TTC TCC AGG CAT TGA CG
T2-HCV	HS-(CH)$_6$–TTT TTC AAC CCA ACG CTA CT
G-HCV	HS-(CH)$_6$–TTT TTC CAA GAA AGG ACC CG
RS1-HCV-c	ATG AGC TCT TTG TCT TCT
G-HCV-c	TTT CGG GTC CTT TCT TGG
T2-HCV-c	AGT AGC GTT GGG TTG

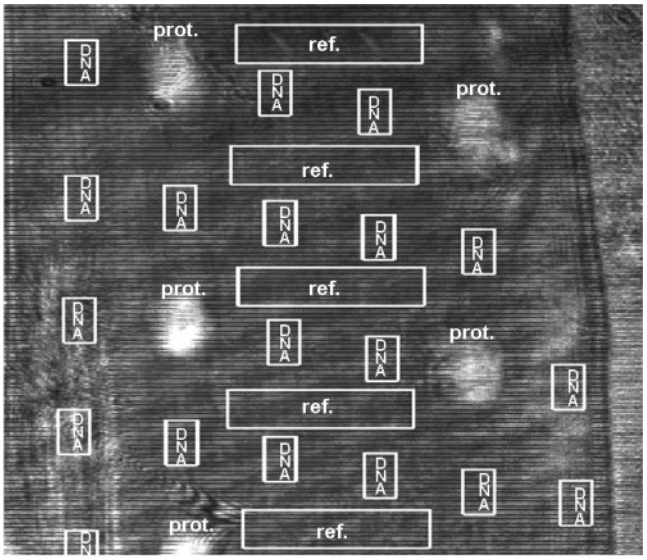

Figure 6. Partial CCD image of a regularly spotted SPR surface. The bright spots are protein markers used for orientation. The small boxes designate the areas where DNA has been immobilized, while the larger, longish boxes are surface areas used for reference measurements.

position of the clearly visible protein spots, 32 detection areas were placed on the surface to measure binding events in the DNA spots. Additionally, nine reference areas were designated between the DNA spots. Five of them can be seen in Figure 6. The references were used to correct the signals from the DNA spots for changes of the refractive index of the buffer, for example, due to temperature drifts, and to compensate intensity variations of the laser beams.

The size of each DNA detection area was 18 × 42 pixels on the CCD. Taking into account that about 25% of the surface was covered with DNA spots, it should be possible to measure simultaneously about 400 spots with the present arrangement if the whole CCD chip area would be used. Unfortunately, our present software does not allow recording the data of more than 50 boxes simultaneously.

Hybridization Measurements. The measured intensity in different areas varied by up to 20% due to an inhomogeneous intensity distribution. This causes a sensitivity difference in different areas which should be taken into account by the data interpretation. A buffer solution with the addition of 0.3% NaCl was pumped through the flow cell for about 1 min. The value of the signal caused by this solution was used for normalizing the sensitivity in individual areas.

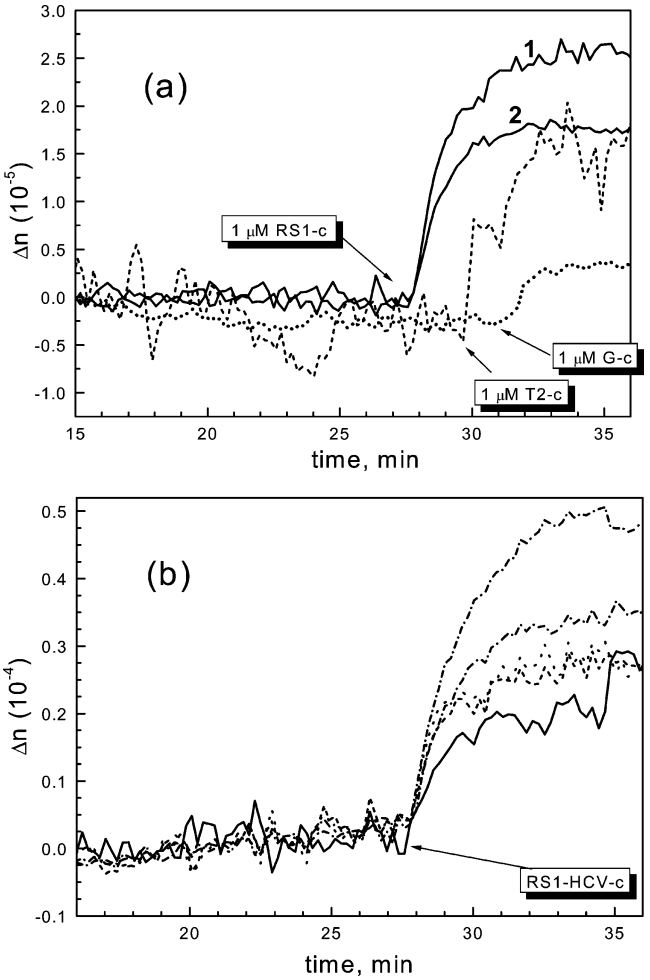

Figure 7. (a) Hybridization of DNA's RS1 (1) and RS2 (2) by RS1-c and of T2 and G by T2-c and G-c, respectively. In all cases, the DNA concentration in the buffer was 1 μM. (b) Simultaneous hybridization of the same oligonucleotide (RS1-c) in five different spots.

1 μM RS1-HCV-c, 1 μM T2-HCV-c, and 1 μM G-HCV-c were pumped through the flow cell one after another for about 5 min. In between, buffer was pumped through the flow cell.

According to DNA in the buffer, hybridization signals were observed in the corresponding DNA spots on the surface. The number of boxes set for the measurements of RS1, RS2, T2, and G were 5, 4, 8, and 5, respectively, and the signals of the spots representing the same DNA were averaged.

Figure 7a shows the averaged hybridization signals in the RS1 spots as well as in the RS2 spots when RS1-c is injected. These oligonucleotides differ only in one base, so that the signals represent a perfect match (a) and a single mismatch (b). The signal of the perfect match is higher than the signal of the single mismatch. This shows the possible application for SPR imaging in single nuclear polymorphism (SNP) analysis.

The hybridizations by T2-c and G-c are also displayed in Figure 7a. The onsets of the hybridizations are about 2 (T2-c) and 4 min (G-c) later than for the RS1 spots. The signals have been shifted in time for better display in Figure 7a. The baseline noise and the noise of the hybridization signal of the T2-HCV spots (dashed curve) were much larger than the noise contribution in the other signals. The reason for this is not known. One reason might be that the T2 spots are arranged directly behind the protein spots according to the buffer flow direction. Rebinding of the protein molecules could be a reason for the higher noise in the T2 spots.

Twenty-five images were taken for each data point to minimize the camera noise and to reduce the detection limit. The time between two subsequent data points of the hybridization curves was about 12 s since the integration time of an individual image was 0.5 s. The noise level was determined by taking into account the background measured over 10 min before the onset of the hybridization. For example, the noise measured in all five RS1 spots separately revealed a mean noise for a single box which is equivalent to $\Delta n = 1.5 \times 10^{-6}$. The signals used for the evaluation of the detection limit are shown in Figure 7b. It has to be stressed that the shot noise of the camera was still the limitation of the detection power (noise level $\Delta n = 0.7 \times 10^{-6}$). The scattering of the hybridization signals from spot to spot was large as can be seen in Figure 7b. It is an indication that the immobilization procedure with the spotter needs improvement.

The detection limits can be improved by taking more spots into account. For example, a noise signal which corresponds to $\Delta n = 6 \times 10^{-7}$ was measured when all five RS1 spots were integrated. The dominating limitation was still the shot noise of the camera which was equivalent to $\Delta n = 3 \times 10^{-7}$.

The hybridization signals measured in the present investigation were about 5 times smaller than in our earlier experiment where the immobilization of the DNA was done manually.[10] Therefore, it is likely that the signal can be boosted again if the immobilization procedure with the spotter is improved. Further improvements can be expected using a longer immobilization time and a higher DNA concentration in the spotting process. The volume of one spotter drop was about 17 nL. Even if all molecules in a drop are immobilized, the maximum density on the surface is only 5×10^{12} molecules/cm^2 using 1 μM DNA. This is about 2 times smaller than the saturated monolayer density reported in refs 15 and 16.

CONCLUSION

A new differential method for SPR imaging is presented. With two laser wavelengths and a differential image procedure, high-detection power is achieved and high-throughput application is possible. The wavelength pair selection for different analytical requirements was discussed, and the limitations of the detection power of the method were studied. Measurements near to the shot noise limit were carried out. It was shown the present arrangement provides the possibility to measure simultaneously up to 400 reactions at the gold surface with a 3σ detection limit of $\Delta n \approx 5 \times 10^{-6}$. Obtained detection power can be improved by the factor of about 3 at the cost of a smaller linear range by applying other wavelength combinations. Further improvements of the detection power and an increase of the throughput capability can be expected if CCD cameras with higher pixel capacities and a higher readout rate are applied. The future application fields of the new technique will be in particular bioanalyses, genomics, proteomics, and other fields of research and industry where both high-detection power and high-throughput analyses are required.

(15) Yang, M.; Yau, H. C. M.; Chan, H. L. *Langmuir* **1998,** *14*, 6121.
(16) Wolf, L. K.; Gao, Y.; Georgiadis, R. M. *Langmuir* **2004**, *20*, 3357.

ACKNOWLEDGMENT

The authors are grateful for technical help and advice from colleagues of the University of Tübingen (G. Gauglitz and N. Kaeppel), the University of Regensburg (V. Mirzky), and MPI Dortmund (J. Kuhlmann). Financial support by the Ministry of Innovation, Science, Research, and Technology of the state of North Rhine-Westphalia and the Ministry of Education and Research of the Federal Republic of Germany is gratefully acknowledged.

Received for review August 30, 2006. Accepted September 29, 2006.

AC061623J